Biosensors and Bioelectronics 145 (2019) 111677

Contents lists available at ScienceDirect

Biosensors and Bioelectronics

journal homepage: www.elsevier.com/locate/bios

A trimetallic CuAuPd nanowire as a multifunctional nanocomposites applied to ultrasensitive electrochemical detection of Sema3E

Zhiyi Yuan[1], Jun Chen[1], Yilin Wen, Chengli Zhang, Yuan Zhou, Zhangyou Yang, Chao Yu*

Chongqing Engineering Research Center for Pharmacodynamics Evaluation, College of Pharmacy, Chongqing Medical University, Chongqing, 400016, PR China

ARTICLE INFO

Keywords:
CuAuPd
Nanowire network
Semaphorin 3E
Sensor

ABSTRACT

In this work, an innovative metal nanowire-based biosensor designed for the quantitative detection of semaphorin 3E (Sema 3E), a potential biomarker for several diseases such as atherosclerosis and systemic sclerosis, was proposed. For the biosensor fabrication, novel trimetallic CuAuPd nanowire networks (NNWs) were synthesized to utilize as a multifunctional substrate for electron transfer, antibody immobilization and signal amplification via catalyzing the decomposition of hydrogen peroxide. A facile one-step approach was employed at room temperature and atmospheric pressure to synthesize the CuAuPd NNWs, exhibiting advantages of high specific surface area, excellent electron transport property, superior catalytic property, and excellent biocompatibility. Cyclic voltammetry (CV), electrochemical impedance spectroscopy (EIS) and atomic force microscopy (AFM) was examined to determine the successful fabrication process of the sensor, while the electrochemical method of amperometric i-t curve was used for the detection of target. The results demonstrated accepted stability, excellent selectivity, sensitivity and accuracy, which displayed a linear range of the analyte concentration that covered 100 fg mL^{-1} to 10 ng mL^{-1}, with a low detection limit of approximately 1.5 fg mL^{-1} (S/N = 3), achieved under optimum conditions. This result suggests that the sensor could be applied to the serum samples for Sema 3E quantitation.

1. Introduction

As well-known molecules initially characterized by their roles in regulating axon guidance, semaphorins and their receptors (plexins) are soluble cell-surface proteins that contribute to the process of morphogenesis in multiple organ systems though their effects on cell morphology, proliferation, differentiation and migration (Tamagnone et al., 1999; Sakurai et al., 2012). More recent evidences indicate that one member of this family, semaphorin 3E (Sema 3E) plays crucial regulating roles in axon guidance, vascular patterning, and immune regulation. The serum level of soluble Sema 3E shows high correlation with several metabolic and immunological diseases, such as atherosclerosis, obesity and systemic sclerosis (Qin et al., 2017; Shimizu et al., 2013; Mazzotta et al., 2015). Therefore, Sema 3E as a potential biomarker or sign for multiple disorders, could be used as an important noninvasive target for pathologic diagnose or therapeutic monitoring. Thus, an effective technology to detect the Sema 3E is required.

The analytical methods which have been employed to measure Sema 3E expression so far are mainly immunoassays including enzyme-linked immunosorbent assay (ELISA), western blot (WB), immunohistochemistry (IHC) (Movassagh et al., 2017; Casazza et al, 2010, 2012). These immunoassays have been widely used for their high sensitivity and selectivity as classical strategies for protein quantification. Nonetheless, they suffer from several deficits including but not limited by low accuracy, time-consuming, the dependence of sophisticated operation and expensive equipment. Moreover, the level of Sema 3E associated with diseases generally range from 100 pg mL^{-1} to 10 ng mL^{-1} (Qin et al., 2017; Kwon et al., 2015). However, current quantitative immunoassays which are available commercially are mostly capable of quantifying Sema 3E at the nanogram per millilitre level (Mazzotta et al., 2015; Kwon et al., 2015). Thus, an effective point-of-care technique for rapid, high-throughput detection at low cost and low concentration is required. In recent decades, electrochemical immunosensors have attracted great attentions and shown great promise to be utilized as effective methods for protein quantification based on a variety of nanomaterials to produce large improvements in detection speed, sensitivity and accuracy (Ghindilis et al., 1998). However, there has been no electrochemical sensor developed for the measurement of Sema 3E yet.

The ideal biosensors with potential application prospect should

* Corresponding author. College of Pharmacy, Chongqing Medical University, 1 Yi Xue Yuan Road, Chongqing, 400016, PR China.
E-mail address: yuchao@cqmu.edu.cn (C. Yu).
[1] Zhiyi Yuan and Jun Chen contributed equally to this work.

https://doi.org/10.1016/j.bios.2019.111677
Received 11 June 2019; Received in revised form 3 September 2019; Accepted 4 September 2019
Available online 06 September 2019
0956-5663/

have the properties of good specificity, sensitivity, accuracy, repeatability, wide measurement range, as well as easy operation, rapid sensing and low cost (Rezaei et al., 2016). However, sensors with excellent performance of electrochemical detection are often complicated in the process of material synthesis and sensor fabrication, which restricts their practical applications. Therefore, more novel nanomaterials characterized by multifunctional properties and unsophisticated synthetic process are needed to simplify the sensor fabrication. In this work we synthesized a new trimetallic material of CuAuPd nanowire networks (NNWs) by a similar one-step one-phase chemical reduction reaction at room temperature and pressure without capping agents and surfactants, which was modified and developed from the synthetic method for CuPtPd NNWs reported before (Hong et al., 2016). The prepared CuAuPd NNWs exhibited the extraordinary structure of nanowire networks, displaying high specific surface area, excellent electrocatalytic performance and electroconductibility, as well as good ability to immobilize bio-recognition molecules. As previously reported, ultrathin NNWs formed by Pt or Pd are effective electrocatalysts due to their outstanding electrocatalytic performance and enough space to accommodate more biomolecules compared with membranous and spherical nanomaterials (Guo et al, 2011, 2013). However, the high price of Pt and Pd inhibits their wide application. Cu, as a cheap and abundant transitional element, was introduced into the nanowire to reduce the consumption of Pt and Pd to lower the cost, which was also demonstrated to be able to assist the generation of NNWs, tune the electrocatalytic property as a catalyst and enhance the electric conductivity as previously reported (Saleem et al., 2013; Yin et al., 2012; Hong et al., 2015). The Cu-contained Pt or Pd NNWs exhibit excellent electrochemical properties. Nonetheless, their poor ability to immobilize bio-recognition molecules stands as a major obstacle to hinder their applications. To solve the problem, we introduced Au element which exhibits good biocompatibility and permits easy immobilization of biomacromolecules onto the NNWs to help bind more antibodies via the strong coordination bond of Au-NH_2 interaction between nitrogen atoms and Au atoms (Xiao et al., 1999; Lei et al., 2003; Ran et al., 2010; Hu et al., 2016). The multiple excellent properties including electroconductibility, antibody immobilization, and signal amplification which are integrated in one material and simple synthetic process of the novel trimetallic CuAuPd NNWs underpins their possible wide use for electrochemical detection as both of modified and signal materials.

In the present study, we developed an immunosensor based on the CuAuPd NNWs for quantitative detection of Sema 3E with a simple and facile protocol. Compared with other traditional immunoassays, the immunosensor displayed the advantages of high sensitivity and specificity, good reproducibility, acceptable stability, broad linear range and low detection limit, as well as operational simplicity, low cost, which increased the possibility of commercialization of the immunosensors practically and economically. Furthermore, analytical performance of the sensor was successfully employed in human serum samples. In addition, the CuAuPd NNWs could be extensively utilized in the sensors for the evaluation of other significant biomarkers in pathologic diagnosis.

2. Materials and methods

2.1. Chemicals

A human Semaphorin-3E (Sema3E) ELISA Kit(CSB-EL020984HU) was purchased from Cusabio Biotech (Wuhan, China, www.cusabio.com). Copper chloride ($CuCl_2$), Gold (III) chloride trihydrate ($HAuCl_4{\cdot}4H_2O$), and sodium tetrachloropalladate (Na_2PdCl_4) were bought from Sigma-Aldrich (USA, www.sigmaaldrich.com). Bovine Serum Albumin (BSA), $K_3Fe(CN)_6$ and $K_4Fe(CN)_6$ were obtained from Beijing Chemical Reagents Company (www.crc-bj.com). Dopamine, L-cysteine and glucose were ordered from Aladdin (www.aladdin-e.com). All the reagents were of analytical reagent grade and used without further purification. Human serum of healthy people was provided by the First Affiliated Hospital of Chongqing Medical University (http://www.hospital-cqmu.com). Sodium phosphate buffered saline (PBS) was prepared and used as the buffer for detection. Ultrapure water (> 18.2 MΩ) purified by a Millipore Mill-Q purification system was utilized throughout the experiment.

2.2. Apparatus and measurements

The images of biometric nanomaterials CuAu, CuPd, and the trimetric nanowire networks (NNWs) CuAuPd were acquired by transmission electron microscopy (TEM, S-4800, Hitachi, Tokyo, Japan). The composition of the prepared CuAuPd nanowire network was determined by Energy dispersive X-ray spectroscopy (EDS) performing on a JEOL JSM-6700F microscope equipped with a collector. X-ray photoelectron spectroscopy (XPS) and X-ray diraction spectroscopy (XRD) was respectively recorded on Thermo Scientific Escalab 250Xi and BRUCKER D8. Atomic force microscopy (AFM) images were performed by Bruker Dimension icon (USA). The electrochemical experiments, including cyclic voltammetry (CV), amperometric i-t curve and electrochemical impedance spectroscopy (EIS) were measured by a CHI660E electrochemical workstation (Chenhua Instruments Co., Shanghai, China) using a conventional three-electrode system containing a reference electrode (saturated calomel electrode, SCE), a counter electrode (platinum wire) and a working electrode (glassy carbon electrode, GCE).

2.3. Preparation of CuAu, CuPd, and CuAuPd NNWs

CuM NNWs were synthesized as previously described with some subtle changes (Hong et al., 2016). For CuAuPd NNWs, 6 mg of $NaBH_4$ was dissolved in 3 mL of H_2O, and the freshly prepared $NaBH_4$ solution was diluted by 15 mL of water in a 50 mL breaker. And then an aqueous mixture prepared by dissolving 1.94 mg Na_2PdCl_4, 3.32 mg of $CuCl_2$ and 93.32 μL of $HAuCl_4$ (5%) into 2 mL of water was injected into the above $NaBH_4$ solution in 15 s under vigorous stirring at a rate of 500 rpm using a magnetic stirrer at room temperature. After about 10 min, the reaction was finished and visible precipitation formed. The reaction solution was transferred into an EP tube of 2 mL. Then the prepared CuAuPd NNWs were collected and washed with water for 3 times. The precipitation was dried in vacuum oven overnight.

The CuAu NNWs and CuPd NNWs were also synthesized in a similar way, which differed in the amount of $NaBH_4$ (4 mg $NaBH_4$ dissolved into 2 mL H_2O) and the corresponding metallic precursors, that is to say, only Na_2PdCl_4 and $CuCl_2$ was added for CuPd NNWs synthesis, or only $CuCl_2$ and $HAuCl_4$ for CuAu NNWs.

2.4. Fabrication and measurement procedure of the electrochemical biosensor

The fabrication procedure of the electrochemical immunobiosensor for Sema3E is illustrated in Scheme 1. In order to obtain a mirror-like surface for better modification, the glassy carbon electrode (GCE, Ø = 4 mm) was polished with 0.3 and 0.05 μm alumina powder sequentially followed by ultrasonic cleaning in ultrapure water, absolute ethanol and then ultrapure water again successively for 5 min each step. Then the aqueous suspension of CuAuPd NNWs (10 mg mL^{-1}) was dropped onto the dry surface of the electrode and formed the membrane after air-dried at room temperature. Subsequently, 10 μL of a Sema3E antibody solution was cast on the modified electrode surface and further incubated at 10 °C overnight to combine antibodies with CuAuPd NNWs via the strong coordination bond of Au-NH_2 interaction between Au in the NNWs and NH_2 in the antibodies. After the reaction finished, the electrode was rinsed with ultrapure water to wash away unbonded antibodies and then incubated with 0.25% BSA for 30 min at room temperature to block nonspecific binding sites. Before the target

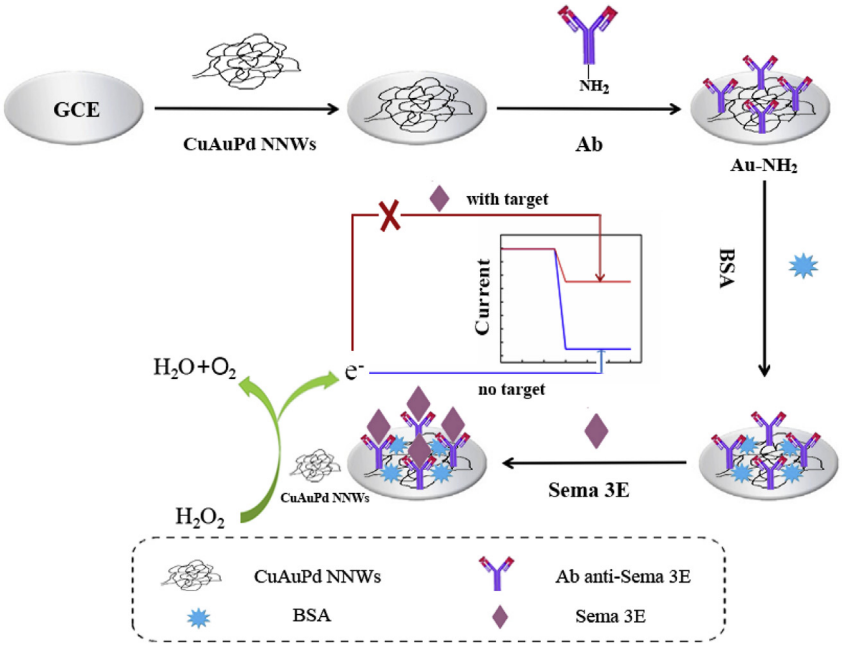

Scheme 1. Schematic representation of the electrochemical immunosensor of Sema 3E.

detection, the modified immunosensor was stored at 4 °C. Finally, 10 μL of the solution containing different concentration of the Sema3E antigens was added onto the modified biosensor and kept at 37 °C for 2 h. An amperometric i-t curve was performed in PBS (pH = 7.5) with 1 mmol L^{-1} H_2O_2 to measure the amount of the analyte. The H_2O_2 solution was freshly prepared right before the detection to prevent the effect from the concentration decrease of H_2O_2.

2.5. Electrochemical measurements

To verify the successful modification of the electrode, CV and EIS measurement for each electrode fabrication steps were performed in 5 mmol L^{-1} $[Fe(CN_6)]^{3-/4-}$ solution. To perform the electrochemical response changes after the analyte combination, the amperometric i-t curves were recorded at -0.4 V in PBS (pH = 7.5) with H_2O_2 at room temperature.

3. Results

3.1. Characterization of CuAuPd NNWs

The morphology of the prepared CuAuPd nanomaterial synthesized with our newly developed and modified method was characterized by TEM. As shown in Fig. 1A, TEM image of CuAuPd presented a typical structure of NNWs, displaying a feature of mutual crisscross and adhesion, consistent with previous study on CuPtPd NNWs (Hong et al., 2016).

Energy Disperse Spectroscopy (EDS) was used to further determine the composition of CuAuPd NNWs. The result of EDS showed the NNWs contained full of the three elements Cu, Au and Pd (Fig. 1B). This fact could be supported by X-ray photoelectron spectroscopy (XPS), because of the presence of the characteristic peaks Cu 2p, Pd 3d and Au 4f, for the three atoms (Fig. 1C). Furthermore, as shown in the XPS spectra of Pd and Au, they seemed to be mainly existed as Pd^0 and Au^0, since no obvious shoulder peaks were observed in Pd 3d and Au 4f (Fig. S1B&C). However, the presence of Cu^{2+} was indicated by the peak identified as Cu 2p3/2 sat, even though Cu^0 or Cu^{+1} was the overwhelming majority (Fig. S1A). Moreover, the XRD spectrum of CuAuPd NNWs displayed the typical characteristics of face-centered-cubic (fcc) nanostructure (Fig. S2) (Hong et al., 2016). In addition, the data of CV performed in a 0.5M H_2SO_4 solution scanning from 0 to 1.6 V (vs. SCE) also verified the successful synthesis of CuAuPd NNWs, for the CuAuPd showed the characteristic peaks of both Au and Pd at ~0.85 V and ~0.25 V (Fig. 1D and Fig. S3). These results confirmed the successful synthesis of CuAuPd NNWs.

3.2. Choice of the CuAuPd NNWs

In order to optimize the electrochemical performance of Cu-contained NNWs, in which Cu was essential for the formation of special structure of NNWs (Hong et al., 2016), a comparation was carried out between CuAuPd NNWs, CuPd NNWs and CuAu NNWs.

Amperometric i-t curve, a common electrochemical method for catalytic activity analysis was performed to record the current responses produced by H_2O_2 which could be decomposed to H_2O and O_2 by electrochemical catalysis of the trimetallic CuAuPd NNWs. Compared with CuAu, CuAuPd and CuPd NNWs showed better electrochemically catalytic activity in a H_2O_2 solution at −0.4 V (vs. SCE) (Fig. S5A). This result suggested that Pd displayed much more excellent catalytic activity than Au in the CuAuPd NNWs. Moreover, TEM images showed that CuAu NNWs exhibited shorter and thicker network nanostructure than CuAuPd and CuPd NNWs (Fig. S4), which may decrease the specific surface area and superficial active atomic ratio, exhibiting lower atomic utilization and weaker catalytic activity (Li et al., 2018). On the other hand, as seen in Fig. S5B&C&D, the i-t responses of CuAuPd and CuAu NNWs showed more significant decrease after incubation with antibody at the same concentration, suggesting that they had immobilized more antibody molecules. Therefore, the Pd and Au may mainly contribute to the catalytic activity and its ability to capture biomolecules respectively. These results indicated that the novel trimetallic CuAuPd NNWs which displayed better catalytic activity and ability to immobilize more biomolecules than bimetallic CuAu and CuPd NNWs was confirmed to be an optimal nanomaterial for immunosensor fabrication.

To detect the electroactive surface area of CuAuPd NNWs, we recorded CVs of the CuAuPd NNWs modified electrode at different potential scan rates in the solution of 5 mM $[Fe(CN_6)]^{3-/4}$ (Fig. S6). The electroactive surface area was calculated to be 25.08 mm^2 for CuAuPd NNWs modified electrode and 12.61 mm^2 for bare electrode according to the Randles-Sevcik equation (Xie et al., 2015). The result illustrated

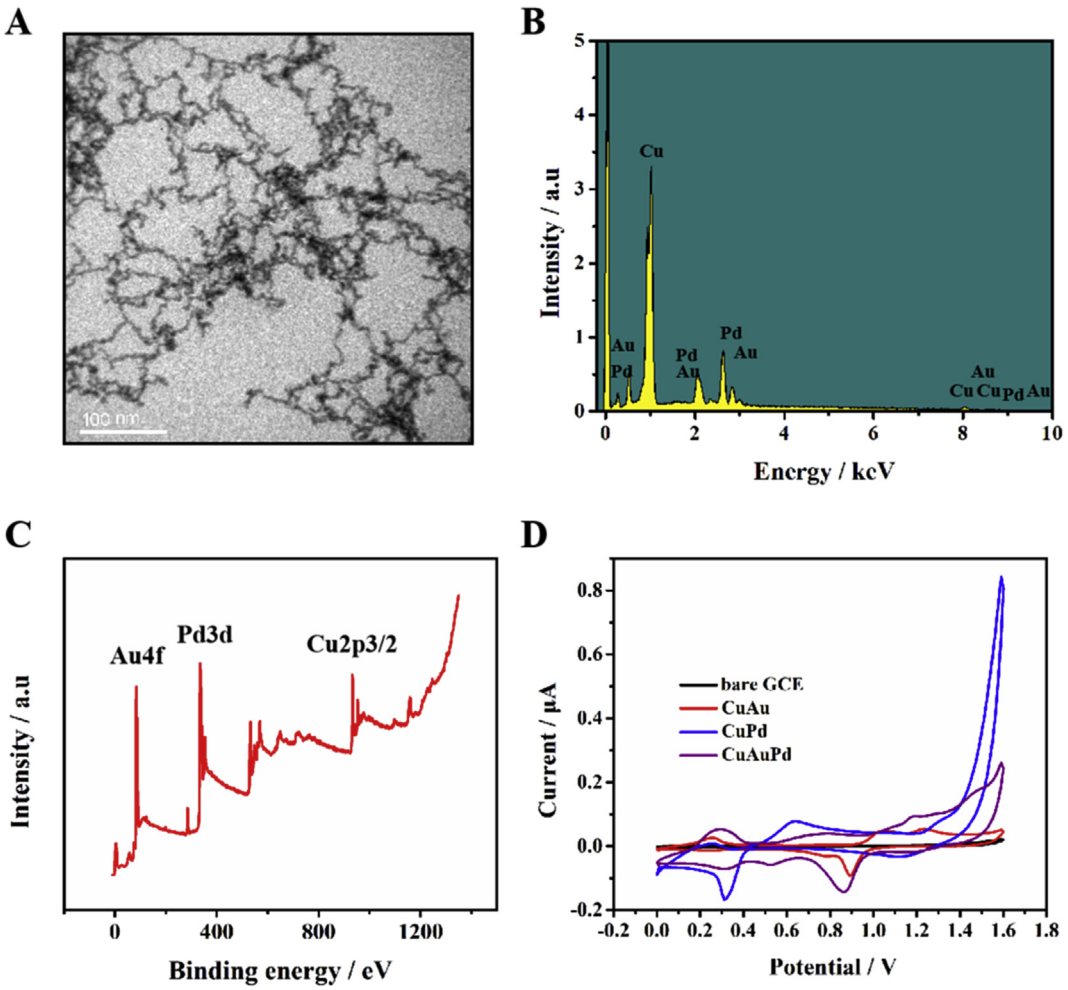

Fig. 1. TEM image of CuAuPd NNWs (A); EDS of CuAuPd NNWs (B); XPS of CuAuPd NNWs (C); CV curves for a bare GCE, CuAu, CuPd, and CuAuPd NNWs measured in 0.5 M H_2SO_4 at 50 mV s^{-1} (D).

that the prepared CuAuPd NNWs could improve the surface area, as well as conductivity of the biosensor.

3.3. Characteristics of modified electrodes

By fitting the need of monitoring the fabrication process of the proposed immunosensor, the data of CV, EIS for the stepwise modified electrode were collected in a solution of 0.1 M KCl containing 5 mmol L^{-1} $[Fe(CN)_6]^{3-/4-}$ as a redox probe (Fig. 2 and Table S1). The parameters of EIS were a 5 mV amplitude and a frequency range from 10^{-3} to 10^{-5} Hz at room temperature, while the CV measurements were performed from −0.2 to 0.6 V (vs. SCE) at a scan rate of 50 mV s^{-1}. Moreover, amperometric i-t curves was used for further confirmation.

Fig. 2A shows how CV responses changed in the processes of different electrode modifications. Dominantly, the oxidation peak current after CuAuPd NNWs was dropped onto GCE surface (curve b) was much higher than the corresponding peak of bare GCE (curve a). Whereas,

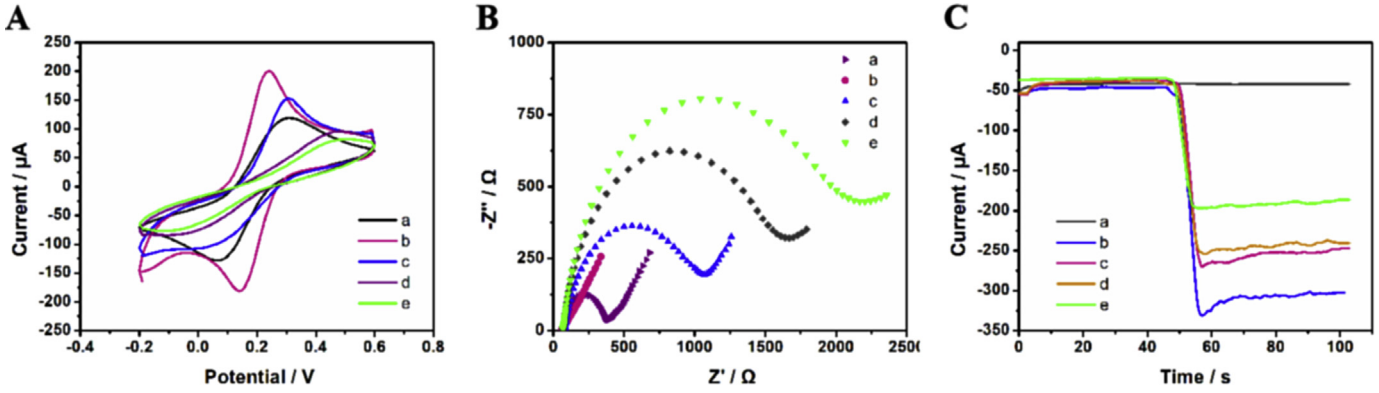

Fig. 2. CV (A) and EIS (B) of stepwise modified electrodes in 5 mM $[Fe(CN)6]^{3-/4-}$ solution containing 0.1 M KCl; Amperometric i-t curves of a bare electrode (a), CuAuPd/GCE (b), Ab/CuAuPd/GCE (c), BSA/Ab/CuAuPd/GCE (d), and specific recognition with Sema 3E (e) recorded in PBS (pH = 7.5) with 1 mmol L^{-1} H_2O_2 (C).

after anti-Sema 3E antibodies were successively immobilized on the electrode via Au-NH_2 affinity (curve c), the peak current decreased drastically, suggesting that the non-conductive layer of proteins severely impeded the electron communication. And the peak current decreased continually after the immunosensor was incubated with BSA for blocking the remaining nonspecific active sites (curve d) and objective antigen molecules (curve e) for detection in sequence, which was originated from sluggish diffusion of the redox probe toward the electrode surface impeded by proteins as a kind of biomacromolecules.

As another common technique for electron-transfer resistance detection, the impedance responses were recorded and depicted in Fig. 2B. The parameter $R_{ct,}$ short for charge transfer resistance which was represented by the diameter of semicircle was used for digital comparison. R_{ct} reduced obviously after CuAuPd NNWs were added onto the bare GCE electrode corresponding to the excellent electrical conductivity of the CuAuPd NNWs (curve b). However, after antibodies, BSA and finally analytes were added onto the electrode step by step, R_{ct} showed a significant increase (curve c, d & e). These observations were in agreement with the preceding results obtained from CV and amperometric i-t responses (Fig. 2C), verifying the successful fabrication of the immunosensor.

In addition, AFM was employed to characterize the topology and roughness of the stepwise modified electrode surface. The surface after deposition of CuAuPd NNWs exhibited larger height of 90.25 nm and root mean square roughness Rq of 12.722 nm (Fig. 3A), than bare GCE surface (Image not shown). Then the values of height and Rq significantly increased to 149.32 nm and 20.85 nm respectively after antibodies were deposited on the surface (Fig. 3B), which indicated that amounts of antibodies were covalently immobilized to the modified surface leading to a much rougher surface. When the electrode surface was blocked by BSA, the value of height increased to 168.54 with a slight drop in the value of Rq to 19.878 nm (Fig. 3C). This could be explained by preferential binding of BSA with free non-specific interfacial sites rather than spots occupied by the antibody molecules, resulting in the decrease of the surface roughness. After the final step of antigen detection, the AFM topography image showed the highest and roughest surface, with height of 201.15 nm and Rq of 24.710 nm, due to the recognition and binding of antigens to antibodies (Fig. 3D). These results were consisted with the conclusions obtained from CV, EIS, and amperometric i-t curves, and validated that the biosensor was successfully fabricated sensor once again.

3.4. Optimization of experimental conditions

To obtain the optimum results, several parameters that influenced the biosensor fabrication or the electrochemical reactions were optimized during the experiment, including concentration of CuAuPd NNWs, concentration and immobilization time of anti-Sema 3E antibody, pH of PBS, and the incubation time of Sema 3E antigen. As shown in Fig. S7, the respective results illustrated that the best signals were achieved when the experimental conditions of Sema 3E detection were (A) 10 μL of 1 mg mL^{-1} CuAuPd NNWs for electrode modification, (B) incubation in 10 μL of a hundred times diluted antibody (C) for 10 h at 10 °C for immobilization, (D) incubation in 10 μL antigen at 37 °C for 2 h, and (E) analysis in PBS at pH 7.5.

3.5. Analytical performance of the electrochemical biosensor

Under the optimum conditions, the proposed immunosensor was applied for the quantitative measurement of Sema 3E in serum samples and evaluated by recording of amperometric i-t curves. In the presence of Sema 3E, the electrochemical signal decreased significantly because of the coverage of the surface of the immunosensor which may impeded the electrical conductivity and catalysis effect of CuAuPd NNWs resulting from the poor electron transfer ability of Sema 3E as a kind of protein. As shown in Fig. 4A&B, the value of the current decreased with the addition of Sema 3E molecules, displaying a linear relationship between the current intensity and the logarithmic value of increasing Sema 3E concentrations in the range of 100 fg mL^{-1} to 10 ng mL^{-1}. The linear regression equation was $Y = 10.544\ lgC + 89.759$ with a detection limit of 1.5 fg mL^{-1}, where Y and C represented the value of peak current and antigen concentration respectively. And a correlation coefficient of 0.9987 indicated that the linear relationship was very good.

Compared with other determination methods for Sema 3E (Table 1) and other amperometric immunosensors (Table S2) reported previously, the proposed sensor in this work exhibits a broader dynamic linear range, with a low detection limit than other Sema 3E detection methods and most amperometric immunosensors. However, there are also some immunosensors with the similar sensitivity of fg·mL^{-1} had been reported. But the process of nanomaterial synthesis and sensor construction was much more sophisticated than this work. So, the results indicated that the immunosensor has great potential for the measurement of Sema 3E for the practical applications.

3.6. Repeatability, specificity, and stability of the biosensor

Repeatability, specificity and stability are three key factors for the sensor in the successful development and practical application. The repeatability was studied by five repeated analyzing of the same concentration of Sema 3E using individual proposed immunosensors (Fig. 4C). The relative standard deviation (RSD) of the parallel experiments was 1.7166% indicating the excellent repeatability of the sensor.

The specificity of the sensor was estimated at first by choosing glucose (Glu), L-Cysteine (L-Cys), ascorbic acid (AA), BSA, dopamine (DA) as interferential species (Fig. 4D). The results showed that 100 pg mL^{-1} of Sema 3E led to a substantial decrease in the amperometric (i-t) response. However, compared with blank or target analyte Sema 3E, the changes in the current intensity were insignificant and negligible in the presence of 80 μg mL^{-1} glucose, 100 ng mL^{-1} other interferents or the mixture, suggesting that the sensor could be applied to quantitative determination for Sema 3E specifically.

To evaluate the stability of the sensor, the amperometric i-t response for target analysis under the same condition was collected using the constructed sensors after stored at 4 °C for different time, lasting for 28 consecutive days (Fig. S8A). The results showed that the current response decreased less than 1.2% without obvious changes during the first week. After 4 weeks storage, about 91% of its initial current intensity was retained. Moreover, when the fabricated sensors were tested under consecutive cyclic voltammetry scans for 50 cycles in 5 mmol L^{-1} $[Fe(CN_6)]^{3-/4-}$ at a scan rate of 50 mV s^{-1}, the electrochemical signals remained stable. The redox peak current remained more than 94% after 50 laps, revealing good stability for the sensor (Fig. S8B). These results suggested the proposed sensor had great potential for the practical applications with excellent selectivity, repeatability and stability.

3.7. Application for the analysis of serum samples

To evaluate the practical application for analysis of a real sample, the CuAuPd NNWs modified sensor was utilized for the detection of Sema 3E in human serum samples. Different known amounts of Sema 3E were spiked into 50-fold diluted human serum samples to reduce the impurities effect in serum matrix. The samples prepared by this addition method were measured by the proposed immunosensor without any further treatment or purification. The analytical data of the recovery experiments were collected and summarized in Table S3, exhibiting the recovery results ranging from 96.36% to 100% with the RSD less than 4.36%, which indicated that the immunosensor could be utilized in the measurement of complex biological samples to achieve satisfactory results.

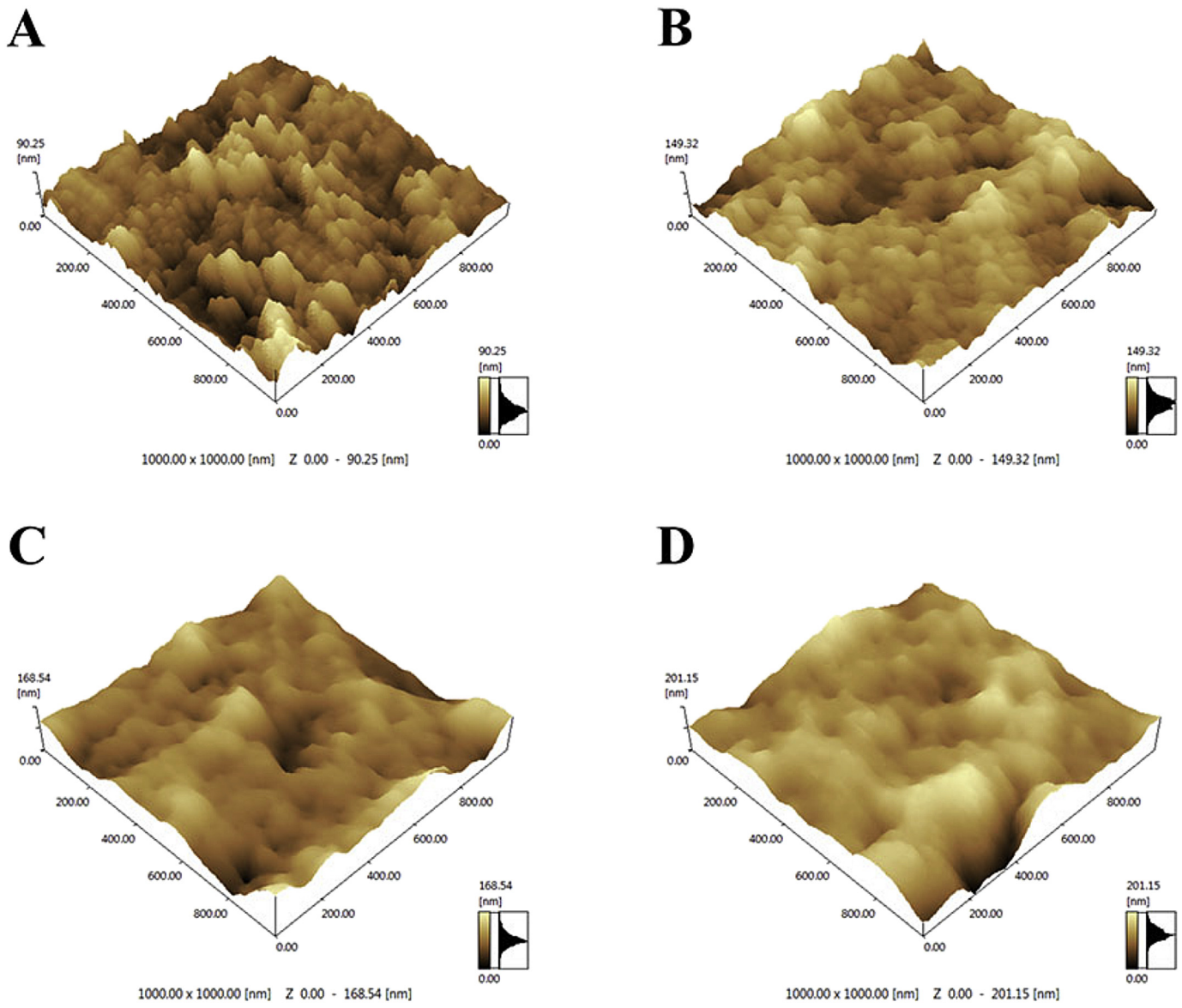

Fig. 3. AFM images of (A) CuAuPd/GCE, (B) Ab/CuAuPd/GCE, (C) BSA/Ab/CuAuPd/GCE, and (D) specific recognition with Sema 3E.

4. Conclusion

In this study, a novel label-free immunosensor for quantitative determination of Sema 3E depended on the CuAuPd NNWs was developed and introduced. CuAuPd NNWs were synthesized at room temperature and atmospheric pressure via a facile one-step method. To design a high performance electrochemical immunosensor, CuAuPd was modified on the electrode, which was utilized not only as a matrix for the immobilization of antibody, but also as the signal material to catalyze the reduction of H_2O_2. The proposed immunosensor exhibited multiple attractive advantages, such as easy to operation, high sensitivity and specificity, good reproducibility and stability with wide linear range and low detection limit, which had promising application in bioassay analysis. However, for clinical medicine application, it is necessary to further improve maneuverability and portability, for example, to use the disposable printed electrodes instead of the conventional electrodes for the point-of-care testing.

CRediT authorship contribution statement

Zhiyi Yuan: Conceptualization, Investigation, Writing - original draft, Funding acquisition. **Jun Chen:** Conceptualization, Methodology, Writing - review & editing. **Yilin Wen:** Data curation, Formal analysis. **Chengli Zhang:** Writing - review & editing. **Yuan Zhou:** Validation. **Zhangyou Yang:** Project administration. **Chao Yu:** Resources, Supervision, Funding acquisition.

Declaration of competing interest

The authors declare that they have no known competing financial interests or personal relationships that could have appeared to influence the work reported in this paper.

Acknowledgments

We thank all the colleagues in our laboratory. This work was supported by Chongqing Basic and Frontier Research Project, China (No.cstc2017jcyjAX0283), China Postdoctoral Science Foundation (No.2017M623305XB), Chongqing Special Foundation for Postdoctoral Research Proposal, China (No.Xm2017021), Chongqing Precision Medical Key Technology Research and Development and Demonstration Projects, China (No.cstc2016shms-ztzx0042) and Youth

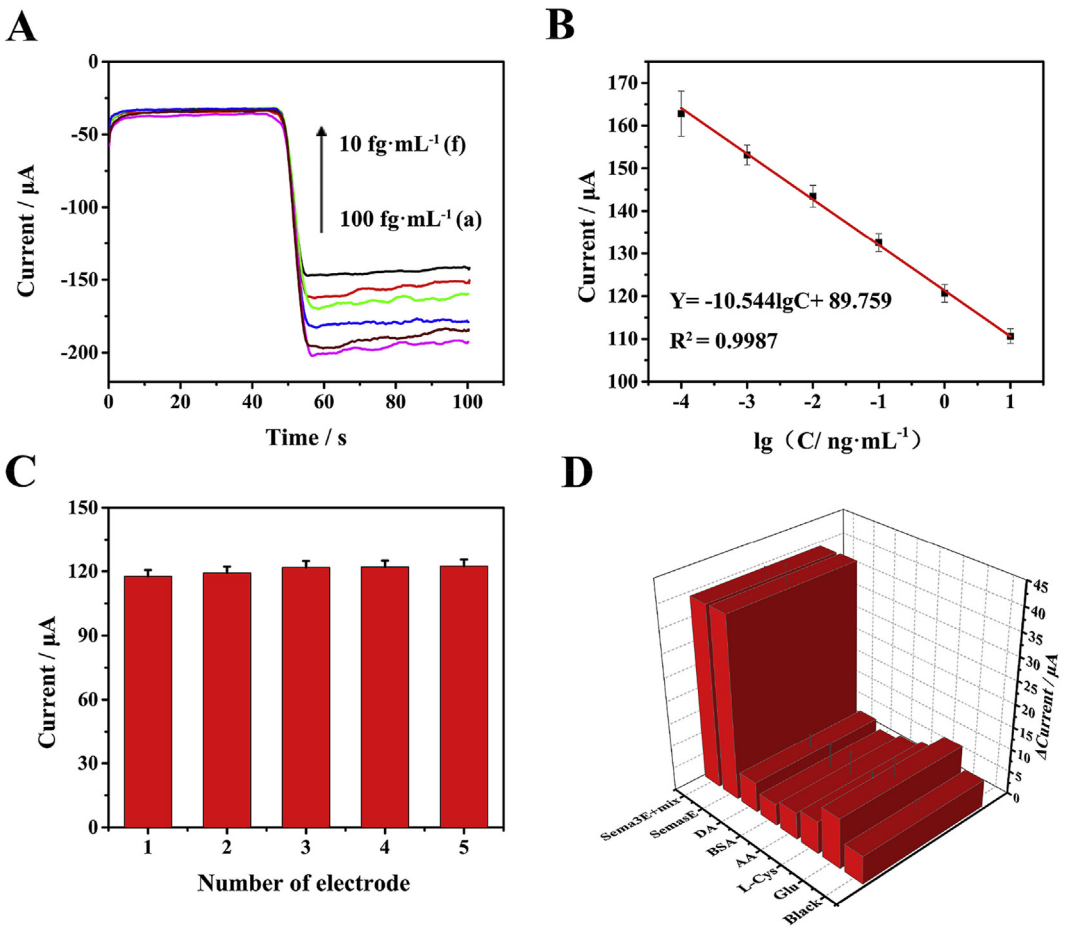

Fig. 4. (A) The i-t curves of the immunosensor for the recognition of different concentration of Sema 3E: (a) 100 fg mL^{-1}, (b) 1 pg mL^{-1}, (c) 10 pg mL^{-1}, (d) 100 pg mL^{-1}, (e) 1 ng mL^{-1}, (f) 10 ng mL^{-1}; (B) The calibration curve of the biosensor toward different concentration of Sema 3E; (C) Reproducibility of 5 different electrodes modified with 1 ng mL^{-1} of Sema 3E; (D) Specificity of the sensor towards: blank without any analyte, 80 μg mL^{-1} glucose, 100 ng mL^{-1} L-Cysteine, 100 ng mL^{-1} ascorbic acid, 100 ng mL^{-1} BSA, 100 ng mL^{-1} dopamine, 100 pg mL^{-1} Sema 3E, and the mixture (100 pg mL^{-1} Sema 3E with 80 μg mL^{-1} glucose, 100 ng mL^{-1} L-Cysteine, 100 ng mL^{-1} ascorbic acid, 100 ng mL^{-1} BSA and 100 ng mL^{-1} dopamine).

Table 1
An overview on recently reported methods for determination of Sema 3E

Detection method	Detection limit	Linear range	Reference
ELISA (Sandwich)	–	0.156 ng·mL^{-1}-20 ng mL^{-1}	Mazzotta et al. (2015)
ELISA (Sandwich)	0.059 ng mL^{-1}	0.156 ng·mL^{-1}-10 ng mL^{-1}	Shimizu et al. (2013)
ELISA (Sandwich)	0.51 ng mL^{-1}	1.25 ng·mL^{-1}-20 ng mL^{-1}	Kwon et al. (2015)
CuAuPd NNWs	1.5 fg mL^{-1}	100 fg·mL^{-1}-10 ng mL^{-1}	This work

Fund of National Natural Science Foundation, China (No.81800389). And We are also grate for the funding from College of Pharmacy, Chongqing Medical University, China (No.YXY2016XSZ01). The authors also acknowledge.

Appendix A. Supplementary data

Supplementary data to this article can be found online at https://doi.org/10.1016/j.bios.2019.111677.

References

Casazza, A., Finisguerra, V., Capparuccia, L., Camperi, A., Swiercz, J.M., Rizzolio, S., Rolny, C., Christensen, C., Bertotti, A., Sarotto, I., Risio, M., Trusolino, L., Weitz, J., Schneider, M., Mazzone, M., Comoglio, P.M., Tamagnone, L., 2010. J. Clin. Investig. 120 (8), 2684–2698.
Casazza, A., Kigel, B., Maione, F., Capparuccia, L., Kessler, O., Giraudo, E., Mazzone, M., Neufeld, G., Tamagnone, L., 2012. EMBO Mol. Med. 4 (3), 234–250.
Ghindilis, A.L., Atanasov, P., Wilkins, M., Wilkins, E., 1998. Biosens. Bioelectron. 13 (1), 113–131.
Guo, S., Li, D., Zhu, H., Zhang, S., Markovic, N.M., Stamenkovic, V.R., Sun, S., 2013. Angew. Chem. Int. Ed. 52 (12), 3465–3468.
Guo, S., Zhang, S., Sun, X., Sun, S., 2011. J. Am. Chem. Soc. 133 (39), 15354–15357.
Hong, W., Wang, J., Wang, E., 2015. Nano Res 8 (7), 2308–2316.
Hong, W., Wang, J., Wang, E., 2016. Nanoscale 8 (9), 4927–4932.
Hu, W., Chen, Q., Li, H., Ouyang, Q., Zhao, J., 2016. Biosens. Bioelectron. 80, 398–404.
Kwon, S.H., Shin, J.P., Kim, I.T., Park, D.H., 2015. Ophthalmology 122 (5), 968–975.
Lei, C.X., Gong, F.C., Shen, G.L., Yu, R.Q., 2003. Sens. Actuators B Chem. 96 (3), 582–588.
Li, K., Li, X.X., Huang, H.W., Luo, L.H., Li, X., Yan, X.P., Ma, C., Si, R., Yang, J.L., Zeng, J., 2018. J. Am. Chem. Soc. 140 (47), 16159–16167.
Mazzotta, C., Romano, E., Bruni, C., Manetti, M., Lepri, G., Bellando-Randone, S., Blagojevic, J., Ibba-Manneschi, L., Matucci-Cerinic, M., Guiducci, S., 2015. Arthritis Res. Ther. 17 (1), 221.
Movassagh, H., Shan, L., Chakir, J., McConville, J.F., Halayko, A.J., Koussih, L., Gounni, A.S., 2017. J. Allergy Clin. Immunol. 140 (4), 1176–1179.
Qin, R.R., Song, M., Li, Y.H., Wang, F., Zhou, H.M., Liu, M.H., Zhong, M., Zhang, Y., Zhang, W., Wang, Z.H., 2017. Ann. Clin. Lab. Sci. 47 (1), 47–51.
Ran, X.Q., Yuan, R., Chai, Y.Q., Hong, C.L., Qian, X.Q., 2010. Colloids Surfaces B Biointerfaces 79 (2), 421–426.
Rezaei, B., Ghani, M., Shoushtari, A.M., Rabiee, M., 2016. Biosens. Bioelectron. 78,

513–523.
Sakurai, A., Doci, C., Gutkind, J.S., 2012. Cell Res. 22 (1), 23–32.
Saleem, F., Zhang, Z., Xu, B., Xu, X., He, P., Wang, X., 2013. J. Am. Chem. Soc. 135 (49), 18304–18307.
Shimizu, I., Yoshida, Y., Moriya, J., Nojima, A., Uemura, A., Kobayashi, Y., Minamino, T., 2013. Cell Metabol. 18 (4), 491–504.
Tamagnone, L., Artigiani, S., Chen, H., He, Z., Ming, G.I., Song, H., Chedotal, A., Winberg, M.L., Goodman, C.S., Poo, M., Tessier-Lavigne, M., Comoglio, P.M., 1999. Cell 99 (1), 71–80.
Xiao, Y., Ju, H.X., Chen, H.Y., 1999. Anal. Chim. Acta 391 (1), 73–82.
Xie, S., Zhang, J., Yuan, Y., Chai, Y., Yuan, R., 2015. Chem. Commun. 51 (16), 3387–3390.
Yin, A.X., Min, X.Q., Zhu, W., Liu, W.C., Zhang, Y.W., Yan, C.H., 2012. Chem. Eur J. 18 (3), 777–782.